# Studies on the Mechanism for the Bimolecular Metathesis Reaction $CH_3 + HCl \Leftrightarrow CH_4 + Cl$

**ZHOU, Zheng-Yu**[*,a,b](周正宇) **CHEN, Guang**[c](陈光) **ZHOU, Xin-Ming**[a](周欣明)
**FU, Hui**[a](傅惠)

[a] *Department of Chemistry, Qufu Normal University, Qufu, Shandong 273165, China*
[b] *State Key Laboratory of Crystal Materials, Shandong University, Jinan, Shandong 250100, China*
[c] *School of Chemistry, Nanjing University, Nanjing, Jiangsu 210008, China*

**The geometry optimization of the transition state, the precursor complex and the successor complex was performed at the 6-311G* basis set level. From the analysis of the vibrational frequency of the precursor complex, transition state, successor complex and the isolated state, the reaction mechanism was derived which was complicated with the bond-rupture electron transfer theory. The atom H in molecule HCl attacks the atom C, forming a transition state via the precursor complex and the electron-transfer happens in precursor complex. And the active energy, electronic coupling matrix element, the reorganization energy, and the reaction rate are obtained.**

**Keywords** DFT theory, bond-breaking, electron transfer, precursor complex

## Introduction

Electron-transfer (ET) reactions have been the subject of many theoretical and experimental studies.[1-3] Some classical and semiclassical, as well as quantum mechanical theories, have been very successful in rationalizing several structure-reactivity relationships and predicting novel features of reactivity. These models established some links between the electron-transfer rate and some parameters such as the activation energy, the reorganization energy, the electronic transmission factor, the nuclear tunneling factor, and so on.

Similarly to the gas phase $S_N2$ reaction, the thermochemistry and kinetics of alkyl radicals are subjects of considerable importance in many fields of chemistry. Kinetic and equilibrium studies of halogenation reactions have been a major source of information on polyatomic free-radical heats of formation. For the chloro system, a quantitative agreement was found between theoretical results and available experimental data.[4] We recall that in a reaction the reactants diffuse toward each other to form a "precursor complex" where they react. Then the reaction leads to a "successor complex" via the transition state and hence by diffusion to the separated products. The central important species in those reactions is the precursor complex. The structures and relevant properties of this precursor complex directly affect the electron transfer mechanism, the rate, and other relevant quantities. In the absence of available experimental data, DFT theory played an auxiliary role in providing relevant information, in helping to elucidate the fundamental aspects regarding this precursor complex and its structural reorganization in the activation process.

In the present study, the BLYP (Becke's 88 exchange functional with the correlation functional provided by Lee-Yang-Parr), the B3LYP (Beck's three parameter functional in conjunction with Lee-Yang-Parr gradient-corrected correlation functions ) method of density functional theory (DFT) and the HF (Hartree-Fock) method, the MP2 (second-order Moller-Plesset) theory are used to investigate the process of reaction. To obtain

* E-mail: zhengyu@qfnu.edu.cn
Received November 14, 2000; revised and accepted May 25, 2001.
Project supported by the National Natural Science Foundation of China (No. 2967305), the Natural Science Foundation of Shandong Province (Y99B01).

the three parameters, the coupling matrix element, the activation energy and the reorganization energy, leading to the rate constants, we focus on computing the equilibrium geometry of the precursor complex and the transition state. The geometries, vibrational frequency, net charge, *etc*. have been optimized in order to discuss the reaction mechanism.

## Theory

*Activation energy and electron coupling matrix*

The reactants and products are isoenergetic (the crossing point of the two non-adiabatic curves is required prior to electron transfer). The transition state is defined as the saddle point along the seam of crossing between two non-adiabatic potential energy surfaces corresponding to the initial and final states of the electron transfer. From Fig. 1, it can be seen that, when the interaction between acceptor and donor is not negligible, the crossing between two curves must be avoided and a $2H_{if}$, separation between the lower and upper curves arises. It represents the energy difference between the crossing activation state (at the crossing point) and the adiabatic activation state (at actual transition state) and thus can be expressed as

$$H_{if} = E_c - E_a \qquad (1)$$

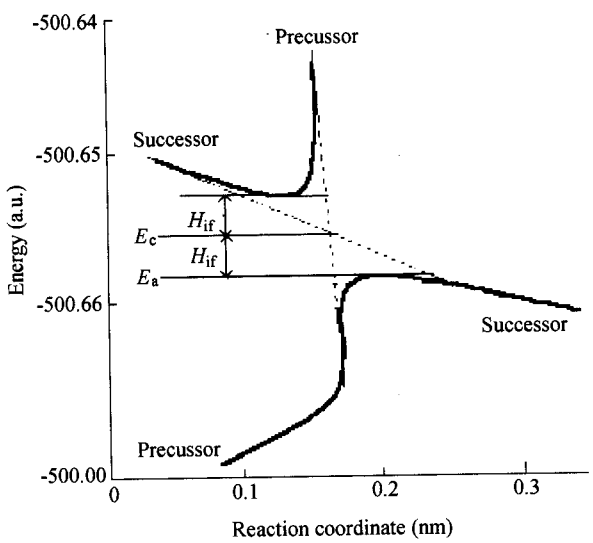


**Fig. 1** Energy profiles of two non-adiabatic states along the reaction coordinate displaying the crossing energy $E_c$ and the splitting of the adiabatic states ($2H_{if}$).

For the precursor complex, the two structural forms are optimized, respectively, using the following three steps: (i) Keeping the optimized geometries of $CH_3$ and HCl, the contact distance $r$ between two species is optimized; (ii) Fixing the optimized contact distance and keeping the C—H distance of the molecular fragment C—H equal to that of the optimized C—H in the isolated state, the C—H in the precursor complex is optimized; (iii) Keeping just optimized contact distance and C—H distance of the molecular fragment $CH_3$ in the precursor complex is defined as the difference between the corresponding precursor complex and isolated species, $CH_3$ and HCl. The transition state is defined as the saddle point along the seam of crossing between the two non-adiabatic potential energy surfaces corresponding to the initial and the final states of the electron transfer, respectively. In this study, our search for the transition state is restricted to the symmetric seam of energy surfaces. The symmetric transition state is obtained as the lowest energy point along this symmetric energy seam. The whole reaction process can be separated into the following five distinct steps:

1. Formation of the precursor complex

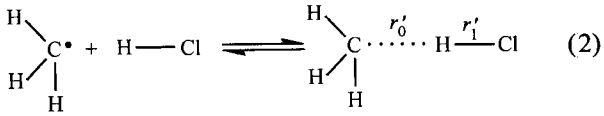

(2)

2. Electron transfer and formation of the transition state

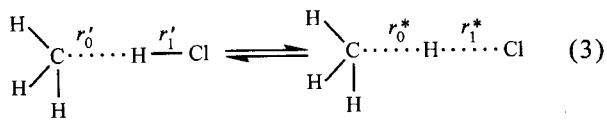

(3)

3. Reorganizaton of the transition state

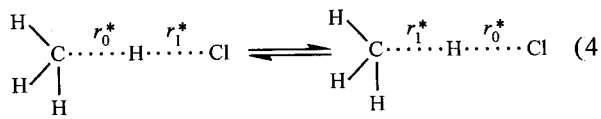

(4)

4. Formation of the successor complex

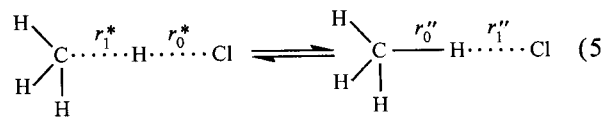

(5)

5. Dissociation of the successor complex

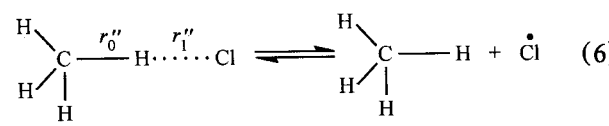

(6)

Then adiabatic activation energy ($E_a$) is easily obtained by subtracting the energy of the precursor complex from the corresponding energy at the transition state, viz.

$$E_a = E_{H_3C\cdots H\cdots Cl(r_0^*, r_1^*)} - E_{H_3C\cdots H\cdots Cl(r_0', r_1')} \quad (7)$$

So, the electronic couple matrix element or the energy reduction caused by the coupling between the initial and the final state of electron transfer may be obtained by Eq. (7).

*Reorganization energy and rate constant*

The λ parameter is the so-called reorganization energy which corresponds to the difference between the free energy of the reactants in their equilibrium configurations (initial state) and that of the products immediately after the electron was transferred (at the nuclear configurations of the reactant equilibrium). The outer-sphere reorganization energy may be accurately calculated via the Marcus theory of nonequilibrium solvent polarization. For a reactant system in the gas phase, the outer-sphere reorganization contribution is virtually zero for weak interaction between the reactants and around medium, and the inner-sphere structural reorganization effect predominates the ET (electron transfer) process. Here reorganization energy can be derived from the expression:

$$\lambda = [f_1 f_2/(f_1 + f_2)] \mid \Delta q \mid^2 \quad (8)$$

where $\Delta q$ can be obtained from the equilibrium values of vibrational coordinate difference between the precursor complex and the successor complex, and the $f_1$, $f_2$ are projected force constants for the precursor complex and the successor complex, respectively. The rate determining step of this reaction is the electron-transfer so that its rate constant can be considered approximately equal to the rate constant of the whole reaction approximately. The dependence of the electron-transfer rate $k$ on some parameters can be expressed as

$$k = \frac{2H_{if}^2}{h}\left(\frac{\pi^3}{\lambda RT}\right)^{1/2}\exp(-E_{ad}/RT) \quad (9)$$

where $h$ denotes the Planck constant and $E_{ad}$ the adiabatic activation energy.

## Calculations

DFT applied the rational correlation through the functions of electron density and gave good descriptions for systems that require sophisticated treatments of electron correlation in the conventional *ab initio* approach. In this study, the geometrical optimizations and electronic structure calculations for the isolated species and the precursor complex are performed with B3LYP, BLYP, HF, and MP2 methods at the 6-311G* basis set level using the Gaussian-94 program package.

## Results and discussion

*Analysis of the vibration modes of the species*

The DFT method is a relatively accurate method to obtain the vibrational frequencies and the vibration modes compared with the *ab initio* method. The vibration modes and vibrational frequencies are listed in Tables 1, 2, and 3 after analyzing the standard orientation and the atom coordination at the 6-311G* basis level. The $CH_3$ alkyl has planar structure and belongs to the point group of $D_{3h}$. Its un-collinear structure makes its freedom number equal to $(3n-6)$, so it has 6 vibration modes. It can be seen that the worst agreement between the calculated and observed results is found in HF/6-311G* calculation. There is a large overestimation of the frequencies at HF level, which may be due to the slightly short bond lengths resulting from neglecting electron correlation in the HF theory. Even the scale factors considering the results are still worse than those by DFT methods. At MP2 level, larger deviations are also found compared with two DFT methods. This indicates that DFT is the relatively superior method for predicting vibrational frequencies. Even though B3LYP is superior to BLYP for many properties, the fact that the BLYP frequencies are closer to observed fundamental vibrational ones has important implications for interpreting observed vibration spectra. As discussed by Rauhut and Pulay,[4] the high level of conformity between BLYP results and the observed fundamental frequencies may be due to error cancellation.

Our geometry optimization indicates that due to slight exaggeration of electron correlation by BLYP method, the BLYP bond lengths are slightly longer than the corresponding B3LYP bond distances. The BLYP

force constants and vibrational frequencies are therefore slightly smaller than the corresponding B3LYP results. As the effect of anharmonicity is also to lower the vibrational frequencies, the high level of conformity between BLYP harmonic frequencies and the observed results is likely to be attributable to the error cancellation by the BLYP method. Therefore, BLYP is a more straightforward and practical approach to deduce the observed fundamental vibrational frequencies for many molecules, the vibration spectra of which are not well understood. The conclusion is as the same as that in our recent work.[5,6] The following discussion of the vibrational frequency is performed at the BLYP/6-311G* level.

The reaction begins with the precursor complex while atom H of the HCl attacks the atom C along the direction vertical to the plane of $CH_3$, and the system has the point group $C_{3V}$ shown in Fig. 2. So the number of vibration modes increased from 6 to 12, then they began to show the vibration modes of the bond H—Cl and the bond H—C produced newly, and the three vibration modes of $CH_3$ stretch vibration were unchanged. For the precursor complex, due to that the H—Cl and C—H bond bendings took place in $CH_3$ free radical, the imaginary frequency would be produced. During the successor complex dissociating to the products, its point group turns into $T_d$ in molecule configuration of $CH_4$, and the number of the vibration modes turns into 9 accordingly as the vanishing of the bond H—Cl. The relationship between the force constant, $f$, and the vibrational frequency, $\omega$, is presented as:

$$f = 4\pi^2\mu c^2\omega^2 \tag{10}$$

where $\mu$ is the reduced mass and $c$ is the light velocity. According to the expression, the force constant is directly proportional to the square of the vibrational frequency from Tables 1, 2, and 3, the vibrational frequency of the bond H—Cl turns from 3103 $cm^{-1}$ which is symmetry stretch in molecule HCl to 1148 $cm^{-1}$ which is asymmetry

**Table 1** Vibrational modes and vibrational frequencies ($cm^{-1}$) of the reactants and the precursor complex

| Species | Symmetry | B3LYP | BLYP | MP2 | HF | Exp.[a] | Assignment |
|---|---|---|---|---|---|---|---|
| Reactants | | | | | | | |
| $CH_3$ | *A2″* | 473 | 478 | 430 | 320 | 606 | $CH_3$ umbrella |
| | *E′* | 1413 | 1378 | 1453 | 1523 | 1396 | $CH_3$ deformation |
| | *E′* | 1413 | 1378 | 1453 | 1523 | 1396 | $CH_3$ deformation |
| | *A1′* | 3105 | 3032 | 3173 | 3242 | 3044 | $CH_3$ sym. stretch |
| | *E′* | 3284 | 3206 | 3366 | 3402 | 3161 | $CH_3$ asym. stretch |
| | *E′* | 3284 | 3206 | 3366 | 3402 | 3161 | $CH_3$ asym. stretch |
| HCl | SG | 2873 | 3103 | 2951 | 3103 | 2991 | HCl stretch |
| Precursor complex | | | | | | | |
| | *E* | i369 | i469 | i352 | 84 | | HCl bending |
| | *E* | i369 | i469 | i352 | 84 | | HCl bending |
| | *E* | 623 | 564 | 585 | 700 | | $CH_3$ rock |
| | *E* | 623 | 564 | 585 | 700 | | $CH_3$ rock |
| | *A1* | 1196 | 1148 | 1192 | 1289 | | HCl asym. stretch |
| | *E* | 1473 | 1430 | 1492 | 1586 | | $CH_3$ asym. deformation |
| | *E* | 1473 | 1430 | 1492 | 1586 | | $CH_3$ asym. deformation |
| | *A1* | 1928 | 1987 | 1282 | 1820 | | CH asym. stretch |
| | *E* | 3158 | 3143 | 3195 | 3211 | | $CH_3$ asym. stretch |
| | *E* | 3158 | 3143 | 3195 | 3211 | | $CH_3$ asym. stretch |
| | *A1* | 3046 | 3029 | 3067 | 3104 | | $CH_3$ sym. stretch |

[a] Data were obtained from Ref.7.

stretch in precursor complex and to i1190 $cm^{-1}$ which is asymmetry stretch in transition state attaining to considerable high energy. It indicated that the force constant is decreased rapidly in this process, and the bond of H—Cl is broken step by step.

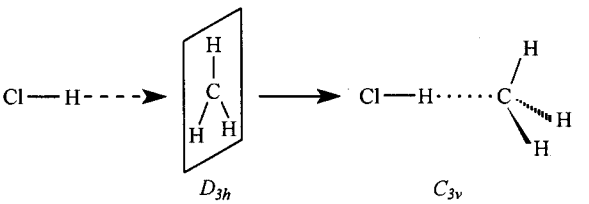


**Fig. 2** Schematic diagram of the reaction of $CH_3$ with HCl.

**Table 2** Vibrational modes and vibrational frequencies of the transition state

| Symmetry | B3LYP | BLYP | MP2 | HF | Assignment |
|---|---|---|---|---|---|
| A′ | i1292 | i1190 | i1208 | i1870 | HCl stretch |
| *A′* | 384 | 341 | 368 | 435 | HCl bending |
| *A″* | 384 | 341 | 368 | 435 | HCl bending |
| *A′* | 545 | 559 | 521 | 450 | CH asym stretch |
| *A′* | 949 | 905 | 911 | 1109 | $CH_3$ rock |
| *A″* | 949 | 905 | 911 | 1109 | $CH_3$ rock |
| *A′* | 1224 | 1203 | 1165 | 1277 | CH sym. stretch |
| *A′* | 1483 | 1455 | 1430 | 1560 | $CH_3$ asym. deformation |
| *A″* | 1483 | 1455 | 1430 | 1560 | $CH_3$ asym. deformation |
| *A′* | 3173 | 3137 | 3025 | 3262 | $CH_3$ sym. stretch |
| *A′* | 3344 | 3312 | 3267 | 3416 | $CH_3$ asym. stretch |
| *A′* | 3344 | 3312 | 3267 | 3416 | $CH_3$ asym. stretch |

**Table 3** Vibrational frequency ($cm^{-1}$) of the products and the successor complex

| Symmetry | B3LYP | BLYP | MP2 | HF | Exp[a]. | Assignment |
|---|---|---|---|---|---|---|
| Successor complex | | | | | | |
| *A*1 | 62 | 48 | 16 | 156 | | HCl out of plane |
| *E* | i149 | i286 | 14 | 247 | | HCl bending |
| *E* | i149 | i286 | 14 | 247 | | HCl bending |
| *A*1 | 1380 | 1319 | 1426 | 1513 | | $CH_3$ rock |
| *E* | 1345 | 1264 | 1428 | 1506 | | $CH_3$ rock |
| *E* | 1245 | 1264 | 428 | 1506 | | $CH_3$ rock |
| *A*1 | 983 | 2954 | 1590 | 1694 | | $CH_3$ asym. deformation |
| *E* | 1555 | 1485 | 1590 | 1694 | | $CH_3$ asym. deformation |
| *A*1 | 3082 | 3057 | 3133 | 3178 | | $CH_3$ sym. stretch |
| *E* | 3136 | 3122 | 3137 | 3186 | | $CH_3$ asym. stretch |
| *E* | 3136 | 3122 | 3137 | 3189 | | $CH_3$ asym. stretch |
| Product $CH_4$ | | | | | | |
| *A*1 | 1354 | 1323 | 1386 | 1469 | 1340 | $CH_3$ rock |
| *E* | 1354 | 1323 | 1386 | 1469 | 1350 | $CH_3$ rock |
| *E* | 1354 | 1323 | 1386 | 1469 | 1350 | $CH_3$ rock |
| *A*1 | 3030 | 2960 | 3078 | 3168 | 3019 | CH sym. stretch |
| *E* | 1582 | 1548 | 1615 | 1605 | 1533 | $CH_3$ asym. deformation |
| *E* | 1582 | 1548 | 1615 | 1605 | 1533 | $CH_3$ asym. deformation |
| *A*1 | 3130 | 3056 | 3214 | 3268 | 3063 | $CH_3$ sym. stretch |
| *E* | 3137 | 3058 | 3215 | 3269 | 3065 | $CH_3$ asym. stretch |
| *E* | 3137 | 3058 | 3215 | 3269 | 3065 | $CH_3$ asym. stretch |

[a] Data were obtained from Ref. 8.

In the successor complex, the vibration mode of H—Cl stretches vanished, and a low frequency that is vibration mode of out-of-plane appeared instead. In the product it disappeared of course. As contrary to the bond of H—Cl, the vibrational frequencies of 1987 $cm^{-1}$ of the bond C—H that is asymmetry stretch and of $-116$ $cm^{-1}$ that is the vibration mode of out-of-plane in precursor complex disappeared in the transition states and the frequency 559 $cm^{-1}$ that is asymmetry stretch of C—H and the frequency 1203 $cm^{-1}$ that is symmetry stretch of C—H bond were produced. It is the process that the three atoms Cl, H and C become collinear and the bond H—C trends to be strong. In the successor complex, the vibration mode of asymmetry stretch vanished and the vibration mode of symmetry stretch became stronger with the affection of the atom C. In the product, the vibrational frequencies of symmetry stretch attained to a rather stable state. In the process of the reaction, the umbrella vibration mode in alkyl $CH_3$ turned into the rock mode of the precursor complex in consequence of the reversal of its configuration just like an umbrella that was deformed by the strong wind, and the frequency of the rock mode was strengthened in transition state and in successor complex in sequence. The deformation vibration mode of the $CH_3$ changed minutely throughout the whole reaction, which shows its relative stability. The vibration modes of the system always affect each other and its result will lead to the changes of the other vibrational frequency. So the nature of the stretch mode of the $CH_3$ decreased in precursor complex because of the affection of its rock mode, but it increased in the transition state after the electron transfer and decreased in the successor complex and product because the net charges were redistributed after the electron-transfer and the reorganization of the structure. When the vibration modes of the $CH_3$ are compared with those of the product, the $CH_3$ rock vibration becomes stronger than before because of the $T_d$ symmetry structure of $CH_4$ produced.

*Process of bond-rupture electron-transfer*

According to the Franck-Condon theory,[9,10] the contact distance and the momentum of atomic nucleus are all unchangeable in one electron transfer process. It took $10^{-16}$ second for the electron transfer to complete. The electron transfers easily in the precursor complex and the transition state. Considering the changes of the frequencies of bond H—Cl and C—H from reactants to the successor complex, it can be seen that the three atoms of C, H and Cl of the whole system have the intention in becoming a linear structure in which the electron transfers rather fast. The electron in the excitative $2\pi$ molecule orbit of HCl has the trend to transfer into the $sp^3$ hybrided orbit of the $CH_4$. Though the electron-transfer happens when the precursor begins to form and the changes of distribution of the electron cloud is a process throughout structural reorganization and disassociation of all middle species in the whole reaction.

*Calulation of rate constant*

To obtain the rate constant of ET reaction, the potential energies of the precursor complex and the successor are scanned in B3LYP/6-311G level. It requires to derive three parameters ($E_a$, $H_{if}$, and $\lambda$) according to Eq. (1), and $H_{if}$, and $E_a$ can be easily calculated from Eq. (1) and (7), respectively. From Eq. (8), $\lambda$ can be derived, so the rate constant can be obtained from the Eq. (9). The results computed in B3LYP/6-311G level are listed in Table 4 where it can be seen that the result of the B3LYP is better in agreement with the experimental value than the results obtained by other methods.

**Table 4** Three parameters ($E_a$, $H_{if}$, and $\lambda$) and the rate constant in 6-311G* level

| | $E_a$ (kJ/mol) | $H_{if}$ ($cm^{-1}$) | $\lambda$ (kJ/mol) | $k$ ($s^{-1} \times 10^{11}$) |
|---|---|---|---|---|
| HF | 13.12 | 312.5283 | 828 | 0.431 |
| MP2 | 13.03 | 284.6178 | 786 | 0.381 |
| BLYP | 13.39 | 305.0075 | 765 | 0.384 |
| B3LYP | 14.42 | 323.9347 | 737 | 0.258 |
| Exp.[a] | 10.626 | | | 0.28 |

[a] The value obtained from Ref.1.

## Conclusion

The reaction mechanism for $CH_3 + HCl \Leftrightarrow CH_4 + Cl$ is studied in this work. Firstly the optimization computation of all kinds of complexes of this system is studied by the DFT method, and it can be seen that the B3LYP and the BLYP methods do well for the computation of frequency. Secondly, the geometry and the various parameters of the precursor complex, successor com-

plex, and transition state are obtained and the bond-rupture electron transfer mechanism of this reaction from the changes in vibrational frequencies is analyzed. Thirdly, to derive the rate constant, three relevant activation parameters ($E_a$, $H_{if}$ and $\lambda$) of the reaction system are discussed, and the B3LYP result is better in agreement with the experimental values.

## References


1 Marcus, R. A. *J. Phys. Chem. A.* **1997**, *101*, 4072.

2 (a) Marcus, R. A. *J. Chem. Phys.* **1956**, *24*, 996.
(b) Marcus, R. A. *J. Chem. Phys.* **1956**, *43*, 679, 3477.
(c) Marcus, R. A. *Faraday Discuss. Chem. Soc.* **1982**, *74*, 7.

3 Zhou, Z. Y.; Xu, J.; Zhang, C. S.; Zhou, X. M.; Du, D. M.; Zhang, K. Z. *J. Mol. Struct.* (*Theochem.*) **1999**, *469*, 1.

4 Rauhut, G.; Pauly, P. *J. Phys. Chem.* **1995**, *99*, 3039.

5 Zhou, Z. Y.; Du, D. M.; Fu, A. P.; Yu, Q. S. *Chin. J. Chem.* **2000**, *18*, 297.

6 Zhou, Z. Y.; Du, D.M.; Fu, A. P. *Vib. Spectr.* **2000**, *23*, 143.

7 Jacox, M. E. *J. Phys. Chem. Ref. Data* **1988**, *17*, 269.

8 Jacox, M. E. *J. Phys. Chem. Ref. Data* **1990**, *19*, 1387.

9 Kohn, G. W.; Sham, L. J. *Phys. Rev.* **1965**, *A140*, 11133.

10 Ziegler, T. *Chem. Rev.* **1991**, *91*, 651.

11 Russell, J. J.; Seetula, J. A.; Senkan, S. M.; Gutman, D. *Int. J. Chem. Kinet.* **1988**, *20*, 759.


(200011244 JIANG, X.H.; DONG, L.J.)